scientific reports

Check for updates

OPEN

Functionalized microcrystalline cellulose crosslinked via diisocyanate-derived urethane bonds for wastewater treatment

Bahia Abu Lail[1], Oudai No'eirat[1], Othman Hamed[1]✉, Waseem Mansour[1]✉, Abdalhadi Deghles[2], Shehdeh Jodeh[1]✉, Motasem Alfar[1], Reem Jalghoum[3], Avni Berisha[4,5] & Omar Dagdag[6]

Copper is a common water pollutant due to its toxicity and widespread presence in various water streams. Various adsorbents have been utilized to remove heavy metal contaminants from water; however, these methods often show limited efficiency and can incur significant costs. This work highlights the synthesis, characterization, and performance evaluation of new crosslinked cellulosic polymers in foam form functionalized with alkylsulfonate moiety for use as efficient adsorbents for copper and other metal ions. Cellulose was first reacted with butane sultone and subsequently crosslinked using p-phenylene diisocyanate and hexamethylene diisocyanate to produce Cell-S-PPF and Cell-S-HMF, respectively. The capacities of Cell-S-PPF and Cell-S-HMF for extracting metal ions from wastewater, along with their optimal adsorption conditions, were evaluated. The Qe values for both polymers were determined to be 19.2 mg/g and 20.0 mg/g for Cell-S-HMF and Cell-F-PPF, respectively. Adsorption proceeded spontaneously at ambient temperature as evidenced by negative Gibbs free energy values. Both polymers showed the ability to quantitatively remove more than 25 metal ions present in a sewage sample, including uranium. Recycling performance shows that Cell-S-PPF and Cell-S-HMF can be recycled by sequential washing with diluted acid and then base, without observable performance loss over at least five adsorption–desorption cycles. The adsorption process obeys the Langmuir isotherm model with a second-order rate. The findings suggest a promising avenue for the commercialization of these materials in wastewater treatment applications. Monte Carlo (MC), DFT, and Dynamic (MD) simulations indicated strong bonding between copper (II) ions and the coordination sites of cellulosic polymers. Since high adsorption negative energy was obtained.

Keywords Urethane, Cellulose, Molecular dynamics, Butane sultone, Wastewater, Metal ions, Isotherm

Wastewater contamination with toxic metal ions and other organic matter is becoming a major issue that poses a global concern, as industrial waste, household items, and agricultural waste are disposed of in the sewer system[1–4]. These waste materials have been identified to release toxic materials into water, including organic matter, dyes, metal ions, and others[5–7]. Examples of toxic heavy metal ions are Cu(II), Cd(II), Cr(III), Zn(II), Hg(II), Pb(II), Co(II), and others. The situation poses a high health risk and requires immediate attention[8,9]. In order to find a solution to this issue, several methods for the removal of metal ions from wastewater have been developed. Among these methods, adsorption has received the maximum attention, as it is not only the most efficient but also a low-cost method used for water purification. In addition, many adsorbents[11–13] are reported in the literature that are suitable for this purpose[10–13]. More attractive absorbents are those that are made from natural based materials since most likely they are safe and recyclable[14–18]. Especially those made from natural macromolecules such as lignin, cellulose and chitosan[19–21]. Even with the quick advancements in natural

[1]Chemistry Department, Faculty of Science, An-Najah National University, P.O. Box 7, Nablus, Palestine. [2]Department of Chemistry, Istiqlal University, Jericho, Palestine. [3]Department of Chemistry, Arab American University, Janin, Palestine. [4]Department of Chemistry, Faculty of Natural and Mathematics Science, University of Prishtina, Prishtina 10000, Kosovo. [5]Materials Science-Nanochemistry Research Group, NanoAlb-Unit of Albanian Nanoscience and Nanotechnology, 1000 Tirana, Albania. [6]Department of Mechanical Engineering, Gachon University, Seongnam 13120, Republic of Korea. ✉email: ohamed@najah.edu; waseem.abuoun@najah.edu; sjodeh@najah.edu

based adsorbents, like those derived from cellulose and nanocellulose, their potential remains unexplored[22–27]. Cellulosic absorbents made from cellulose nanocrystalline (CNC) are promising, but their crystallinity limits access to binding sites[28,29] In addition, cellulose efficiency as an adsorbent is limited due to the availability of one type of binding site, which is a hydroxyl group. Cellulose derivatization with functional groups such as carboxyl, amine, and aryl were among the approaches used for enhancing the affinity of cellulose to metal ions[29]. In another approach, the accessibility was increased by converting cellulose to a composite in foam form. In one instance, this was done by impeding carboxymethyl cellulose (CMC) in a PU matrix and forming a composite[28] The approach was interesting but didn't solve the accessibility, as the cellulose crystalline structure was maintained and the aggregation issue in the cellulose polymer was not resolved. One easy way to address the accessibility problem with cellulose is to convert the crystalline structure of cellulose to a porous structure by introducing a functionality that converts it to foam. Using cellulose derivatives with a group that has a high affinity for metal ions might even be the ideal option.

Foam is known to have unique structures with attractive characteristics that include porosity, controlled pore size, and elasticity. Moreover, foam offers straightforward preparation, exhibits notable stability, and possesses a highly porous structure, which facilitates efficient adsorption and desorption processes at comparatively elevated rates. These properties make it easy to handle, collect, and recycle. These factors make foams an attractive material for use as an adsorbent for metal ions present in wastewater. Recently published research showed the possibility of using PUFs as an adsorbent in wastewater[29–31] Some of the investigated PUFs showed good adsorbent properties; the reasons were related to high surface area, resistance to change in pH, high stability in organic and aqueous solution, and organic mediums[32]. The investigated PUFs were used in a continuous and batch process[33]. PUF with no binding sites for metal ions showed limited efficiency as an adsorbent, it also suffers from limited selectivity[34]. Chemically or physically modified PUF demonstrates improved adsorption rates and selectivity for inorganic and organic substances, including metal ions[35].

In a published work cellulose-based foam was made from polymerizing with amino acid pendant group and diisocyanates. The foam showed excellent affinity for metal ions and removed quantitatively all metal ions present a sewage sample. Kinetic and thermodynamic analyses demonstrated that metal ion binding occurred spontaneously, adhering to a second-order pseudo-adsorption rate.

The use of modified naturally occurring materials as adsorbents for environmental remediation has garnered significant interest, with olive waste biomass being a notable example. Our previously published work demonstrated that olive biowaste contains approximately 45% cellulose polymer. We have developed a method for extracting cellulose from olive biowaste, which involves a two-step process: initial kraft cooking followed by multistep bleaching utilizing various oxidizing agents. In this work, we have shown that these kinds of biomass, which represent wasted resources with significant disposal challenges, can be converted to novel materials capable of removing toxic metal ions from wastewater.

The objective of this study is to transform microcrystalline cellulose extracted from olive waste biomass into a highly porous, cellulose-based foam functionalized with alkyl sulfonate groups. This material is designed to efficiently adsorb toxic metal ions from wastewater. Cellulose microcrystalline, used as a starting material in this work, was isolated from the waste of the olive industry according to a published method[26,27].

Experimental
Material
The chemical and reagents used in this study butane sultone, N,N-dimethylacetamide anhydrous (DMAc), copper(II) nitrate diisopropyl amine, 1,6-hexamethylene diisocyanate, 1,4-phenylene diisocyanate were purchased from a commercial source (Sigma-Aldrich Chemical Company, Jerusalem) and used without any additional purification. All experiments were accomplished using deionized water. Microcrystalline cellulose used in this study was extracted from the olive industry solid waste solid waste by a kraft process and multi bleaching sequence that was developed by our research group[26,27].

Methods
Characterization
The thermal properties of the prepared foam were analyzed using Thermo-Gravimetric Analysis (TGA) with the TG/DSC Star System by Mettler-Toledo. The system was equipped with an HT1100 oven connected to a MX5 microbalance, maintained at a constant temperature of 22 °C. The analysis involved heating the sample from room temperature to 650 °C at a rate of 5.0 °C/mi. FT-IR analysis was conducted using a Nicolet 6700 (Thermo-Fisher Scientific, MA, USA) with a Smart Split Pea micro-ATR accessory. The spectral range was 600–4000 cm^{-1}, with a resolution of 4.0 cm^{-1}, and 256 scans.

The concentration of metal ions following each adsorption experiment was quantified utilizing a Flame Atomic Absorption Spectrometer (FAAS), specifically the ICE3500 AA System by Thermo Scientific, UK. Inductively coupled plasma mass spectrometry (CAP™ RQ ICP-MS) used in this work was purchased from Thermo Fisher Scientific (Waltham, MA, USA) and used in determining the type and concentration of metal ions present wastewater. All adsorption runs were performed in triplicate, and the average value was reported.

Cellulose dissolution and functionalization with alkyl sulfonate (Cell-S)
Cellulose dissolution was carried out in a multistage process. The first stage involved cellulose activation by suspending 4.0 g (0.024 mol of anhydroglucose repeat units) of cellulose powder in 100 mL of distilled water in a round-bottom flask. The suspension was stirred for 2.0 h at room temperature, filtered and suspended in 100 mL methanol, stirred for 1.0 h, and filtered again. The process was repeated two times to ensure the complete removal of water. The operation was repeated twice (2 × 50 mL) with dimethyl acetamide (DMAc) for cellulose activation and methanol removal. The activated cellulose was then suspended in a solution of LiCl (8.0 g) in

DMAc anhydrous (92.0 mL) in a 250 mL round bottom flask. The suspension was stirred until a clear gel was obtained (about 2.0 h).

The gel was treated with 2.52 mL of 1,4-butane sultone 1.9 g (0.014 mol). The mixture was heated at 80 °C for 3 h. Then, diluted with water, the precipitate was collected, washed with excess moisture, and crosslinked with isocyanates as shown below.

Cellulose crosslinking and foam formation

Co-polymerization of cell-S with hexamethylene diisocyanate (Cell-S-HMF) A mixture of Cell-S (5.0 g, 16.3 mmol ahydrogulucose repeat unit, considering DS = 1) was suspended in distilled water (10.0 mL) in a beaker and mixed until a homogeneous suspension was obtained in about one hour. The mixture was diluted with DMAc (10.0 mL), followed by the addition of diisopropyl amine (1.0 mL). 1,6-Hexamethyle diisocyanate (2.3 mL, 2.5 g, 14.0 mmol) was added to the mixture. In about 10 min of stirring at room temperature, an exothermic reaction began, producing foam mass. The collected foam was purified by washing with distilled water (3 × 100.0 mL) and dried at 60 °C.

co-Polymerization of Cell-S with p-phenylene diisocyanate (Cell-S-PPF) The above procedure of making **Cell-S-HMF** was repeated except that p-phenylene diisocyanate was used (2.4 g, 15 mmol) in place of 1,6-Hexamethyle diisocyanate.

Water solubility of foam

A known mass of each prepared foam (1.00 g) was suspended in water (100.0 mL) and mixed for one hour at ambient temperature. The foam was collected by filtration, dried at 110 °C, and weighed.

Adsorption study

Adsorption by batch methods

Copper (II) was selected as model cations in this study. A stock solution with 1000 ppm concentration was prepared from the above cation then diluted to obtain a diluted series of solutions with concentrations ranging from 1.0 to 100 ppm. These solutions were employed to build the calibration curve and investigate the impact of various parameters on the efficiency of foams.

All adsorption experiments were conducted in a 50.0 mL plastic container equipped with a screw cap. The containers were placed in a water bath with a temperature controller. The effect of various adsorption parameters on adsorption efficiency, such as foam dose (mg), metal initial concentration (C_o in ppm), adsorption time (min), solution pH, and temperature (°C) was evaluated. At the end of each adsorption run the suspension was centrifuged (3000 rpm), decanted and the supernatant was analyzed by FAAS at 217.0 nm. The optimum value of each parameter was determined. All tests were run in triplicate, the standard deviation in all reported results was within the range of ± 1.72. All analyses were conducted in triplicate. Data was analyzed using the *t*-test method. Variations were classified as statistically significant when the p-value was less than 0.05.

Thermodynamic and kinetic parameters were determined to assess the nature and mechanism of the adsorption process.

The % removal and the adsorption capacity (Qe, mg/g) were determined using Eqs. (1) and (2)[17].

$$\%\ \text{Removal} = \frac{C_0 - C_e}{C_0} \cdot 100 \tag{1}$$

$$Q_e = \frac{C_0 - C_e}{W} V \tag{2}$$

where C_0 and Ce are the starting and final concentrations of metal ion, respectively. Qe is the equilibrium adsorption capacity in mg/g, W is the weight (mg) of the absorbent, and V is the volume of the solution (L).

Adsorbent regeneration and recycling

Desorption experiments were conducted on foam loaded with Cu(II) ions[36,37], which were collected from the suspension via centrifugation and subsequently rinsed with deionized water. It was suspended in 20 mL glass vials containing 5.0 mL of 0.2 M HCl and 0.01 M EDTA. The mixture was mixed at room temperature for 2 h. After desorption, the recovered adsorbent was treated with 0.05 M NaOH to restore the binding sites. Excess NaOH was removed by rinsing the foam with deionized water several times. The collected foam was subjected to five adsorption–desorption cycles by repeating the same procedure reported above.

Treatment of contaminated water

The adsorption study was performed on a sewage sample obtained from a wastewater plant (Al Awja Treatment Plant) located in city of Jericho, Palestine. The sample was filtered by passing it through a glass sintered funnel under vacuum. Quantitative and qualitative analyses were performed on the sewage sample using ICP-MS (Water Center operated by An-Najah University, Palestine). A 0.5 g sample of each of the prepared foams was loaded in a syringe (5.0 mL). Thereafter, a 20.0 mL sample of the filtered sewage was filtered through the foams during a period of 10 min. The filtrate was collected and reanalyzed by ICP-MS for residual metal ion concentrations.

Computational methods

Computational studies were carried out to provide molecular-level insights into the adsorption mechanisms of Cu(II) ions onto the cellulose-based foams. The methodology consisted of four major stages.

Conformer search and lowest energy structure selection

The initial conformational space of the polymer chains was explored using a random sampling approach. A total of 3000 conformers were generated, and the lowest-energy conformer was selected for further studies. The COMPASSIII forcefield [18] was employed with a convergence tolerance of 1.0×10^{-5} kcal/mol.

Geometry optimization

The selected conformer was subjected to full geometry optimization using the "Smart" algorithm in BIOVIA Materials Studio. Convergence criteria were set at 1.0×10^{-5} kcal/mol for energy, 0.001 kcal/mol/Å for forces, and 1.0×10^{-5} Å for displacement. The COMPASSIII force field was used consistently.

Amorphous cell construction and packing

To simulate bulk polymer behavior, an amorphous cell was constructed containing four polymer chains. The packing density was set to 1.50 g/cc, and the geometry was optimized under periodic boundary conditions. Ring separation, energy checks, and geometry optimization were performed, with the system equilibrated at a bias temperature of 298 K. Loading steps were set at 1000 to ensure optimal packing.

Vacuum layer addition

To simulate adsorption conditions, a vacuum layer of 35 Å was added along the C-axis of the periodic box. Subsequent geometry optimizations were performed to stabilize the system before molecular dynamics (MD) and Monte Carlo (MC) simulations.

Molecular dynamics and Monte Carlo simulations

To simulate adsorption conditions, a vacuum layer of 35 Å was added along the C-axis of the periodic box. Subsequent geometry optimizations were performed to stabilize the system before molecular dynamics (MD) and Monte Carlo (MC) simulations.

Density functional theory (DFT) calculations

To complement forcefield-based simulations, DFT calculations were carried out using the $DMol^3$ module in Materials Studio. The M06-L functional [19] with a double numerical basis set plus polarization (DNP) was used. A self-consistent field (SCF) tolerance of 1.0×10^{-7} Ha was applied, and solvation effects were included using the COSMO model (water). Adsorption energies and quantum theory of atoms in molecules (QTAIM)[20] analyses were performed to quantify the interaction strength and bonding character between Cu(II) ions and the polymer functional groups.

Results and discussion

Functionalization of microcrystalline cellulose and crosslinking

Two cellulosic-based foam containing sulfonate and crosslinked with urethane functional groups were synthesized and applied for the removal of hazardous metal ions from wastewater. The first step involved synthesis of cellulose functionalized with the alkyl sulfonate group Cell-S. This was carried out by reacting a solution of cellulose in LiCl/DMAc with 1,4-butane sultone. In the course of the reaction, the hydroxyl group of cellulose acts as a nucleophile, attacking the δ-carbon atom of 1,4-butane sultone.

Cell-S was reacted with 1,6-hexamethylene diisocyanate and p-phenylene diisocyanate to produce Cell-S-HMF and Cell-S-PPF. The hydroxyl functionalities present on Cell-S react with isocyanate carbons, resulting in the formation of covalent linkages and the generation of amine anions. Subsequent protonation yields urethane linkages (–NH-CO-O–) between cellulose chains. Figure 1 illustrates the reaction scheme for producing the sulfonate-containing cellulose-based foam.

The modification done on cellulose introduced three properties: foam form, ionic functionality, and urethane linkage. These changes enable cellulose to act as an efficient adsorbent for toxic metal ions. The multi-functionality and the high porosity of the prepared polymer enable it to efficiently remove metal ions from wastewater by bonding to them through chelation, ion exchange, and dipole-dipole interaction.

The characterization of Cell-S-HMF and Cell-S-PPF was carried out using FT-IR and SEM. Fourier-transform infrared (FT-IR) analysis verified the effective incorporation of sulfonate and urethane functional groups, whereas scanning electron microscopy (SEM) images demonstrated a spongy, highly porous structure conducive to efficient metal ion adsorption.

FT-IR spectra

The FT-IR spectra of Cell-S-HMF and Cell-S-PPF are presented in Fig. 2a,b, respectively. Both polymers show the N–H stretching vibrations peak with a spike of the NH–CO–O functional group that appears at approximately 3320 cm^{-1}[18]. Cell-HMF shows a C–H stretching peak at 2932 and 2855 corresponding to C–H of hexyl, while Cell-S-PPF shows a peak at 3060 cm which is related to =C–H of the phenyl ring. The peak at 1620.0 cm^{-1} in both spectra refers to the urethane carbonyl. Cell-S-HMF shows two peaks at 1560 and 1530 cm^{-1} can be attributed to the S=O of the sulfonate group. While in the spectrum of Cell-S-PPF they appear at 1570 cm^{-1} as a broad a combination of two merged peaks. The glycosidic linkage (C–O–C) and C–O of alcohol appear as a broad band at 1220 cm^{-1}.

Foam morphology

Images of the surface morphology of the prepared foams Cell-S-HMF and Cell-S-PPF were obtained by SEM. They are shown in Figure 3. The images show spongy and highly porous structures of both polymers. This

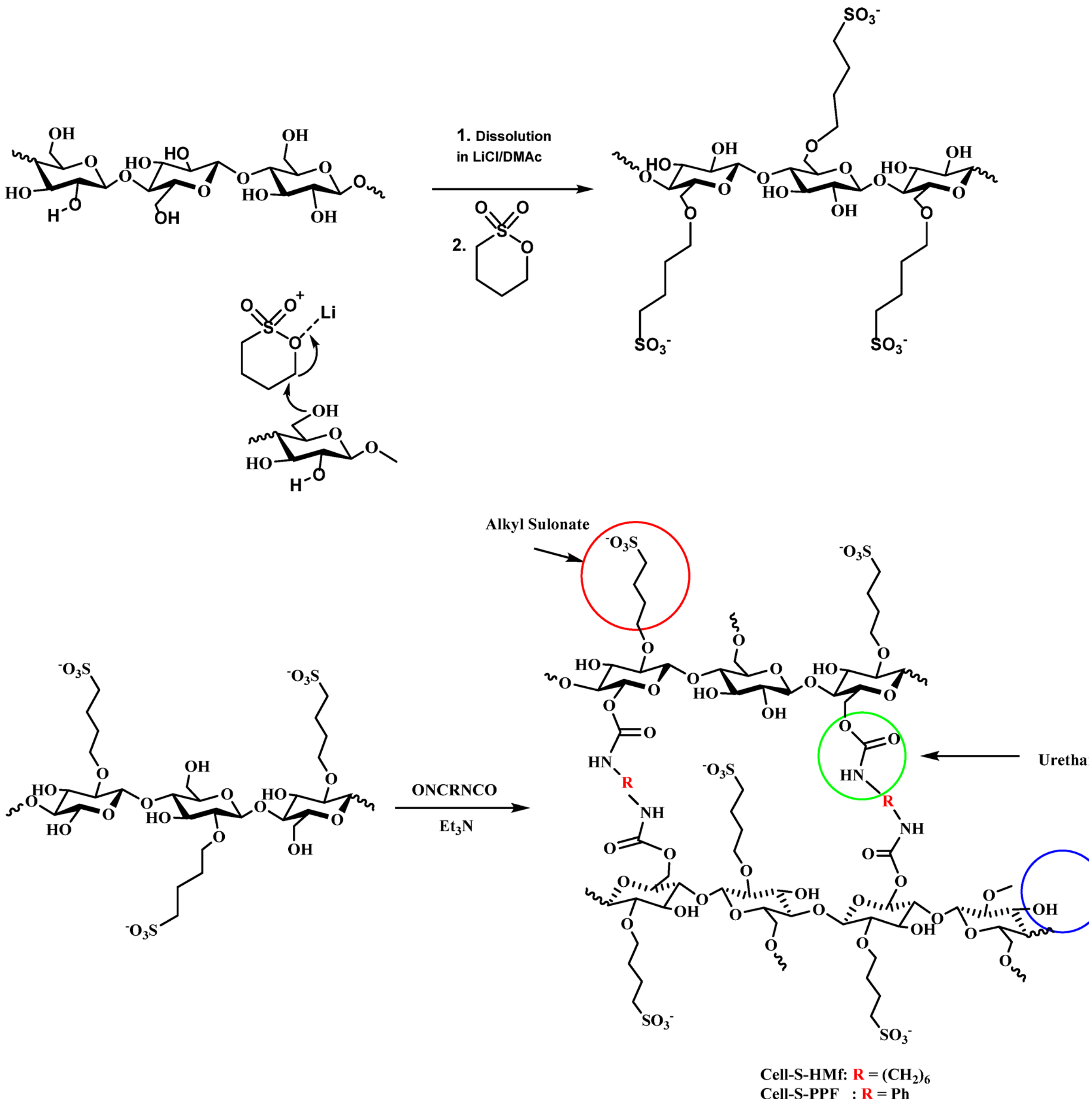

Fig. 1. A schematic diagram shows the synthesis of Cell-S-HMF and Cell-S-PPF starting from microcrystalline cellulose.

could be attributed to the presence of polyurethane (N–CO–O) functionality that holds cellulose chains in a network structure. The spongy structure adds unique properties to the cellulose-based foam, like making it more accessible to metal ions, making it more efficient as an adsorbent and giving it good filtering capability.

Optimum adsorption parameters

The study examined the effects of solution pH, initial metal ion concentration, foam dosage, temperature, and time on the adsorption efficiencies of Cell-S-HMF and Cell-S-PPF. Prior to the adsorption experiments, the solubility of the foams in water was assessed. The results, as indicated in Table 1 below, demonstrate that the foams are insoluble in water.

pH value

Solution pH is a crucial parameter because the pH value has the potential to either activate or hinder the receptor sites abilities to bind metal ions. The study was conducted on a 10.0 mL volume of Cu(II) solution with a 100.0 ppm concentration at room temperature using a 50.0 mg foam adsorbent for 30 min at various pH values. The results are shown in Fig. 4. At a low pH value of about 3.5 the % removal was the lowest for both polymers since at this pH the sulfonate groups are present in their protonated form, which caused their affinity for binding heavy metal to drop. As the pH value increases, however, the sulfonate groups start to shift from acid form to deprotonated form, which converts them to strong chelating agents. The highest adsorption efficiency for both Cell-S-HMF and Cell-S-PPF occurred at a pH range of 6.5 to 8.0. At pH values greater than 9.0, the adsorption

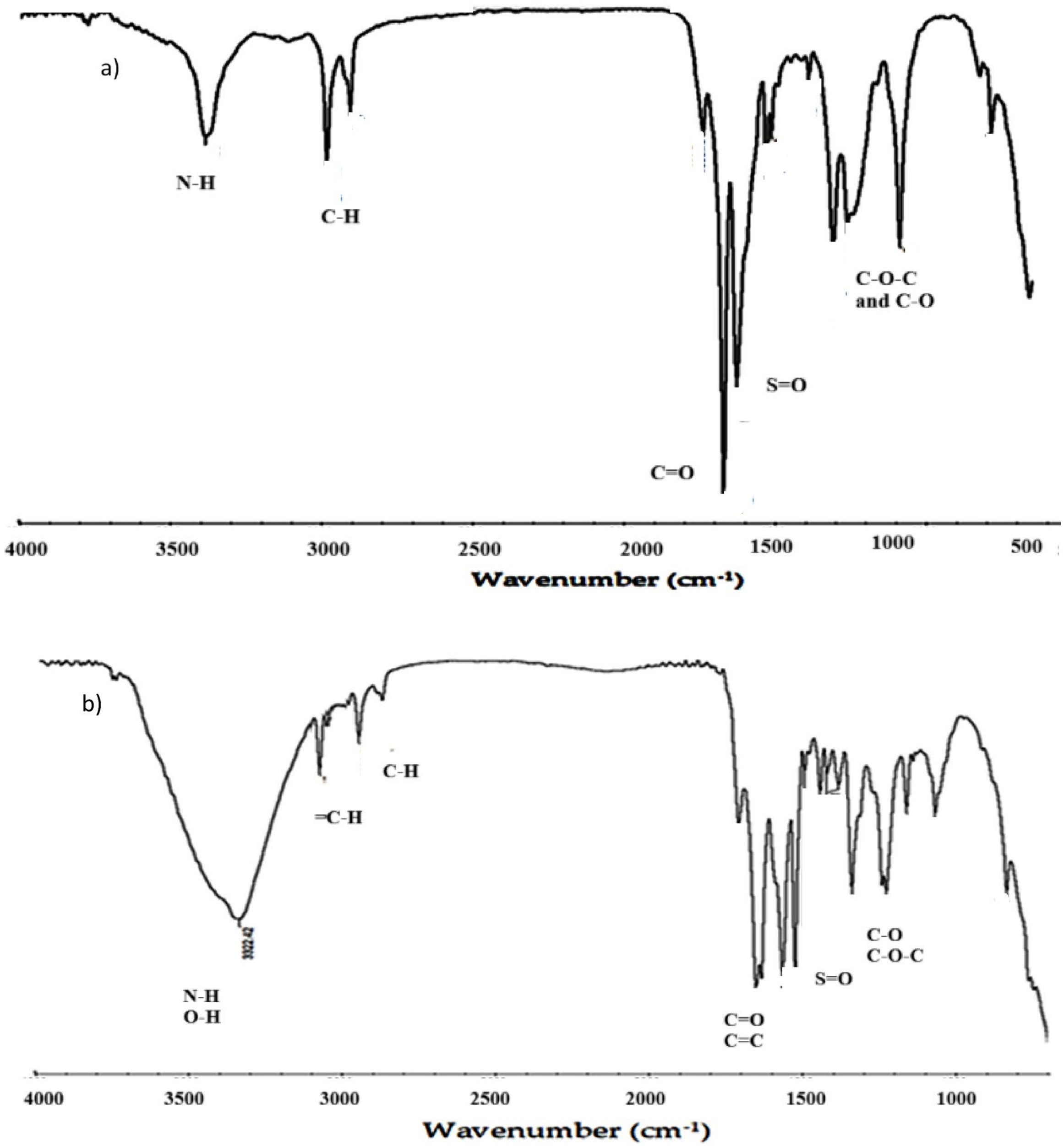

Fig. 2. FT-IR spectra of (**a**) Cell-S-HMF and (**b**) Cell-S-PPF.

efficiency started to decline. This may be due to the formation of metal oxide that dissolves in water-based solutions.

Adsorbent dose

The dependence of Cu(II) removal on the adsorbent dosage is shown in Fig. 5. A study was performed using a 10.0 mL Cu(II) solution at a concentration of 100.0 ppm, maintained at room temperature for 30 min with a pH of 7.5. Increasing the adsorbent dose from 10.0 to 100.0 mg resulted in a reduction of Cu(II) residue from 14.5 to 2.6% for the Cell-S-HMF polymer, and from 10 to 2.01% for the Cell-S-PPF polymer. This can be related to the increase in the number of binding sites at higher absorbent doses. The percentage removal remained nearly constant at approximately 50.0 mg for both Cell-S-HMF and Cell-S-PPF. This outcome is likely due to molecular interactions, such as dipolar and hydrogen bonding between polymer chains, which promote aggregate formation as foam concentration rises. This aggregation reduces the polymer's surface area and limits access to binding sites.

Initial concentration of Cu(II)

The effect of the Cu(II) solution concentration on the adsorption efficiency of Cell-S-HMF and Cell-S-PPF was evaluated while the other parameters, such as pH, solution volume, temperature, time, and adsorbent dose, were

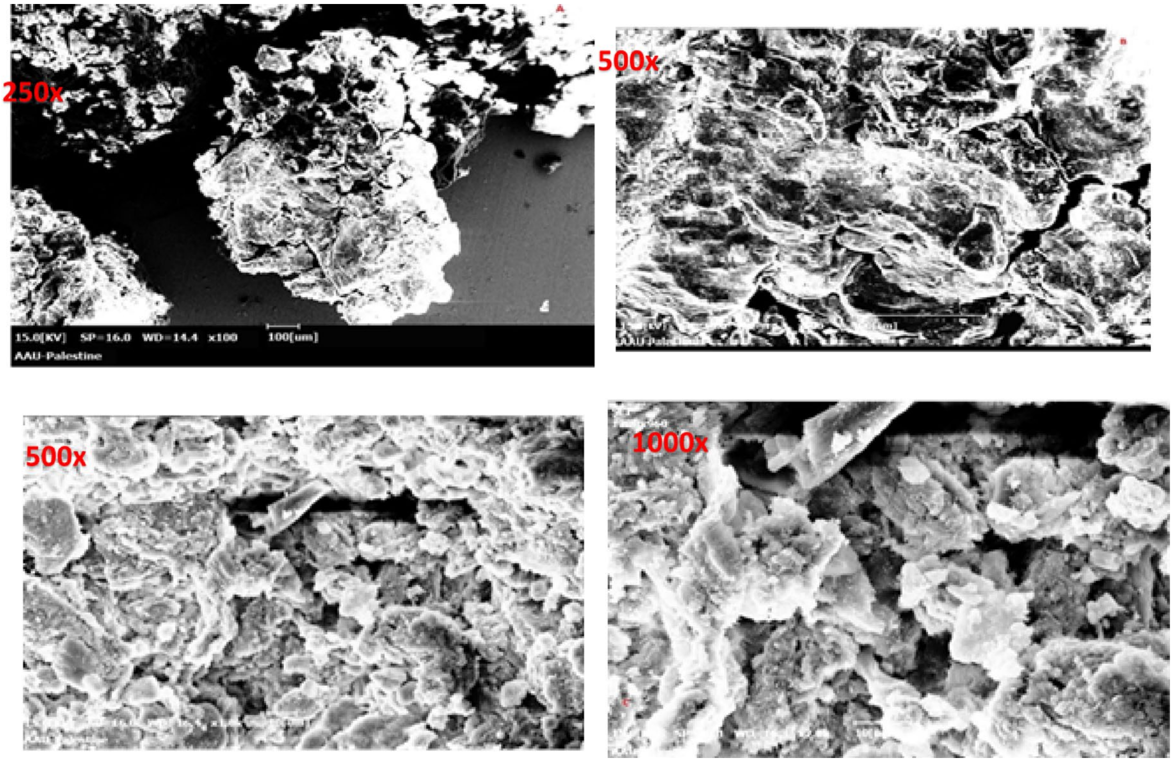

Fig. 3. *SEM images of* Cell-S-HMF at (**a**) 250 and (**b**) 500 × and of Cell-S-PPF *at* (c) *500 × and* (*d*) *1000×*.

Foam	Weight before (g)	Weight after (g)	% Soluble (%)
Cell-S-HMF	1.0	0.98	2.0
Cell-S-PPF	1.0	0.99	1.0

Table 1. Foam solubility results.

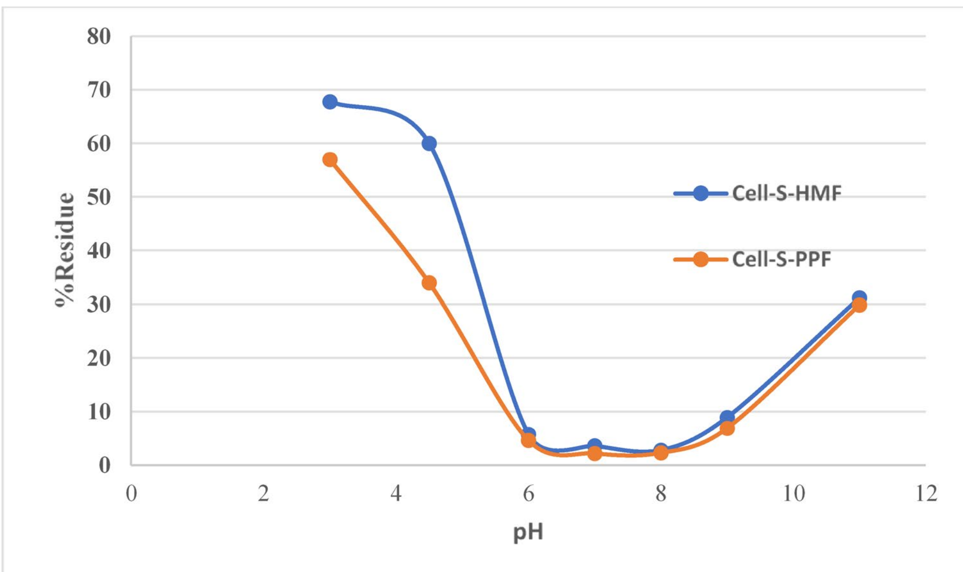

Fig. 4. Effect of pH value on adsorption efficiency of Cell-S-HMF and Cell-S-PPF.

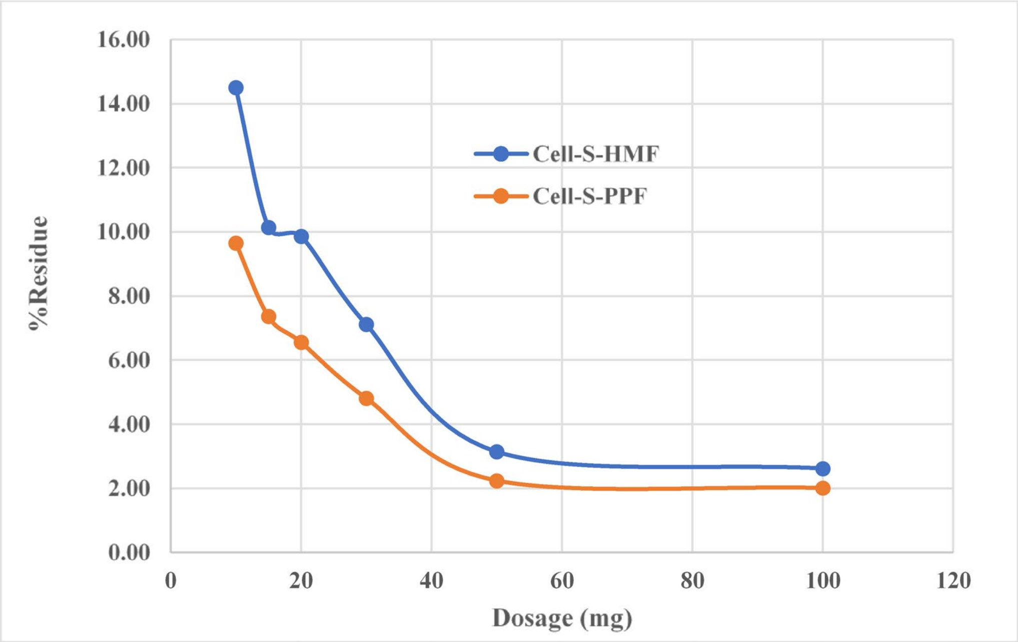

Fig. 5. Effect of Cell-S-HMF and Cell-S-PPF dose on percent removal of Cu(II).

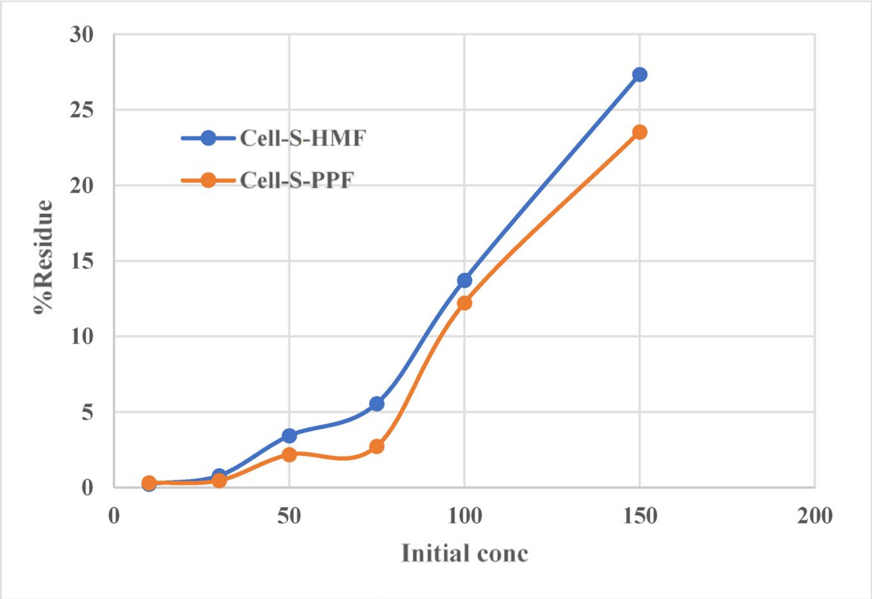

Fig. 6. Effect of Cu(II) initial concentration (C_o) on adsorption efficiency of Cell-S-HMF and Cell-S-PPF.

kept constant at 7.5, 10.0 mL, 25 °C, 30 min, and 50 mg, respectively. The results collected are shown in Fig. 6. The figure shows an increase in the % residue as the initial concentration increases, which could be related to the limited number of metal binding sites on the adsorbent.

Temperature effect
The temperature effect was also evaluated under optimum conditions determined previously. The study was conducted on a 10.0 mL volume of Cu(II) solution with a 100.0 ppm concentration for 30 min at a pH of 7.5. The highest % removal occurred at 25 to 30 °C as shown in Fig. 7. Both foams, Cell-S-HMF and Cell-S-PPF, showed similar behaviors under the effect of temperature, with %removals of over 95% at 25 °C as shown in Fig. 7. The results indicate spontaneous adsorption at room temperature.

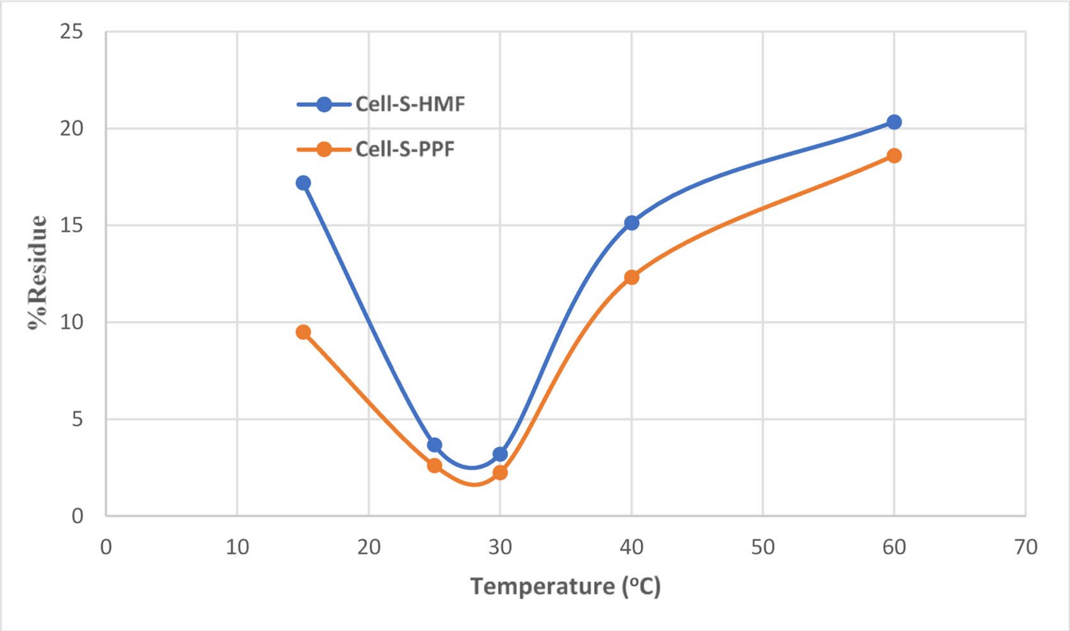

Fig. 7. Temperature effect on adsorption efficiency of and Cell-S-HMF and Cell-S-PPF.

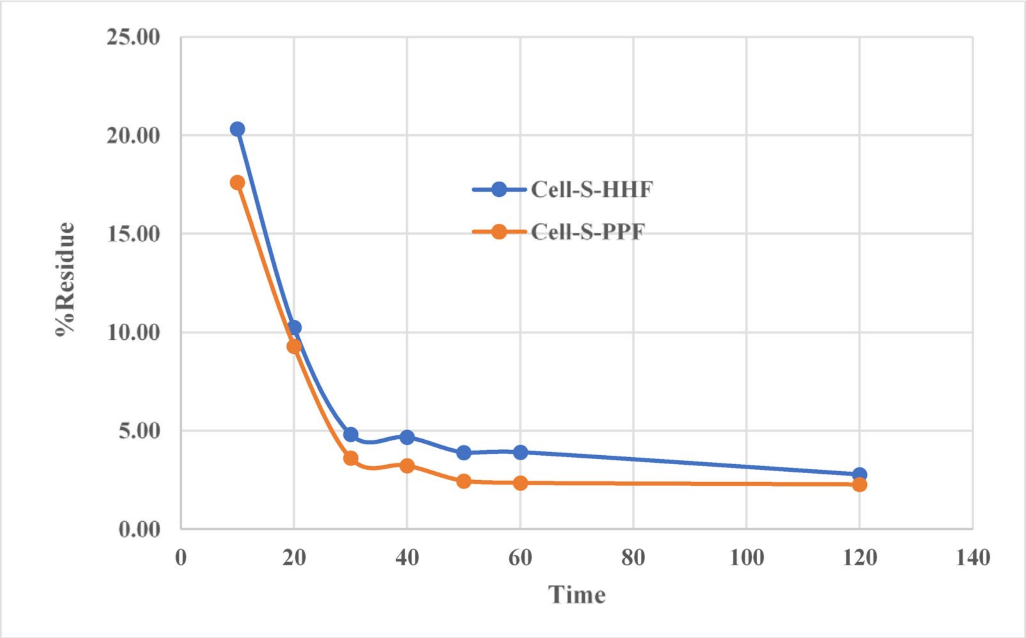

Fig. 8. Effect of contact time (min) on adsorption efficiency of Cell-S-HMF and Cell-S-PPF.

Contact time with adsorbent

The effect of the contact time under predetermined optimum conditions is summarized in Fig. 8. The study was conducted on a 10.0 mL volume of Cu(II) solution with a 100.0 ppm concentration and a pH of 7.5. The % removal of Cu(II) showed an increase as the time progressed. Subsequently, the value stabilized at approximately 30.0 minutes. These results are likely associated with the availability of binding sites at the initial time, which tend to become occupied after about 30 minutes, thereby reaching equilibrium[38]. The high Cu(II) absorption percentages were first related to the abundance of pollutant chelating sites on the external surface of the adsorbent. There is a slight increase in % removal with time then it becomes constant as the equilibrium is attained and the binding sites are occupied.

The following table (Table 2) summarizes the optimum adsorption parameters for both foams, indicating their effectiveness in treating metal contaminants in wastewater.

Adsorption parameters	Cell-S-HMF	Cell-S-PPF
% Adsorption (Cu(II))	96.7% (Qe = 19.2 mg/g)	97.8% (Qe = 20.0 mg/g)
pH	7–8	7–8
Adsorbent Dosage (mg)	50	50
Time (min)	30	30
Temperature (°C)	25	25

Table 2. Optimum adsorption parameters for C(II) and Pb(II) ions.

		% Removal	
Metal ion	Conc. before (ppb)	*Cell-S-HMF*	*Cell-S-PPF*
Ag	17.5	99.6	99.61
Al	1867.3	97.21	97.17
As	3.387	78.38	83.61
B	114.1	86.51	90.63
Ba	71.619	71.24	70.15
Bi	5.000	87.46	83.34
Ca	127,898.3	68.68	67.81
Cd	0.590	97.96	100
Co	2.804	78.03	78.67
Cr	1136.3	89.92	89.97
Cu	76.183	96.01	95.98
Fe	2033.5	93.72	94.14
Ga	1.262	75.99	75.43
K	48,514.8	97.93	98.41
Mg	28,383.7	90.53	96.59
Mn	82.9	56.60	54.71
Mo	5.8	74.92	89.54
Ni	11.6	66.16	66.35
Pb	13.9	96.55	97.31
Rb	31.7	84.08	84.93
Sr	292.0	67.38	66.53
U	1.0	91.77	92.17
V	11.4	53.25	56.48
Zn	214.9	93.24	89.84

Table 3. ICP-MS analysis results on efficiency of Cell-S-HMF and Cell-S-PPF toward various metal ions present in wastewater.

Wastewater purification from metals

A contaminated water sample was obtained from a wastewater treatment plant in Palestine. The samples were treated with adsorbent foam according to the established ideal adsorption conditions. Inductively Coupled Plasma Mass Spectrometry (ICP-MS) was employed to quantitatively determine metal ion concentrations, expressed in parts per million (ppm), prior to and following treatment with the adsorbent foams. The results are presented in Table 3. Both foams demonstrated outstanding adsorption efficiencies for all metal ions present in the sewage sample, including uranium.

Mechanistic investigation of the adsorption process

Adsorption isotherm

To gain detailed insight into adsorption of Cu(II) by the foams Cell-S-HMF and Cell-S-PPF at equilibrium two mathematical models were used Freundlich and Langmuir[31–39].

Results obtained by applying both models are shown in the supplemental file. The R_L value for Cell-S-HMF and Cell-S -PPF is in the range of $0 < R_L < 1$, demonstrating that the adsorption is favorable for both foams. The obtained results show that the two foam adsorbents follow Freundlich model with R^2 values for Cell-S-MMF and Cell-S-PPF are 0.0961 and 0.9898, respectively, it can be concluded that he adsorption process occurs on a heterogonous multilayer surface. More results are shown in supplementary section under Figs. S1 and Table S1.

Adsorption kinetics
A kinetic analysis (supplementary file) on the adsorption of Cu(II) by Cell-S-HMF and Cell-S-PPF was conducted to elucidate the underlying adsorption mechanisms. The pseudo-first order and pseudo-second-order models, commonly used for simulating metal adsorption by various adsorbents, were selected for this purpose[42,43].

Obtained experimental results reveal that the R^2 value for the pseudo-second order (1.0) is higher than that obtained by the pseudo-first order (0.84. 0.89) for Cell-S-HMF and Cell-S -PPF, respectively.

Furthermore, the theoretical q_e values for the two polymers Cell-S-MMF and Cell-S -PPF are 3.23 and 3.76 mg/g which are very close to the experimental q_e values 3.97 and 3.99 mg/g, respectively. The linear characteristics of the resulting graphs, which do not intersect the axes at the origin, suggest that multiple rate-limiting processes could be active during the adsorption phase.

The initial linear trend depicted in Fig. S2 and Table S2 indicates that Cu(II) adsorption onto the cellulose-based foam commences at the polymer surface, where chemical interactions occur between Cu(II) ions and the functional groups present on the foam. The subsequent steps demonstrate linearity, suggesting gradual Cu(II) adsorption and limited intraparticle diffusion rates (Fig. S3) and Table S3. The liquid film diffusion model was more explained in suplimentary section under Fig. S4 and Table S4.

Thermodynamics adsorption of Cu(II) by Cell-S-HMF and Cell-S-PPF
In this work, the thermodynamic parameters entropy (ΔS°), Gibbs free energy (ΔG°) change, and enthalpy (ΔH°) were computed to describe the adsorption process of Cu(II) ions by Cell-S-HMF and Cell-S-PPF polymers, estimate its feasibility, and spontaneity[42]. The determined values of the thermodynamic parameters (ΔS°, ΔH°, and ΔG°) show that the adsorption of Cu(II) by the two foams happened spontaneously and exothermically since all ΔG° values is negative Fig. S5 and Table S5.

DFT calculations
The DMol3 module of the Materials Studio software program was used to compute the interaction energies among the polymer foam (2 chains) and Cu(II) ions. To better comprehend electrical interaction and correlation (DNP)[38,39], the geometrical features of all inhibitors were improved using polarization and a double numerical basis set in combination with the M06-L functional[46]. For the self-consistent field to converge, a change in energy of less than 10^{-7} Ha was required. The screening model (COSMO)[47–49] was employed in this study to describe the impact of water (solvent).

Monte Carlo and molecular dynamic
A Periodic Boundary Condition (PBC) block of the Cell-S-HMF and Cell-S-PPF was generated as a first stage preceding Molecular Dynamic (MD) and Monte Carlo (MC) simulations. the PCB ss shown in Fig. 9 below is composed of 8 chains of the matching adsorbate structures.

Monte Carlo (MC) can be employed to predict the interactive strength between adsorbent foam and Cu(II) in the adsorption process. In this study, a computational model was utilized to predict the strength of the interaction between cellulose-based foam and Cu(II) ions. The box model employed for these calculations had dimensions of 20.53 Å inside length and 55.54 Å in height. The MD and MC computations were performed inside of a simulation box that contains 710 molecules of water and a single Cu(II) ion. Inc calculation of the MD and MC COMPASSII forcefield was followed [50–64]. The following settings were employed in the MD: NVT

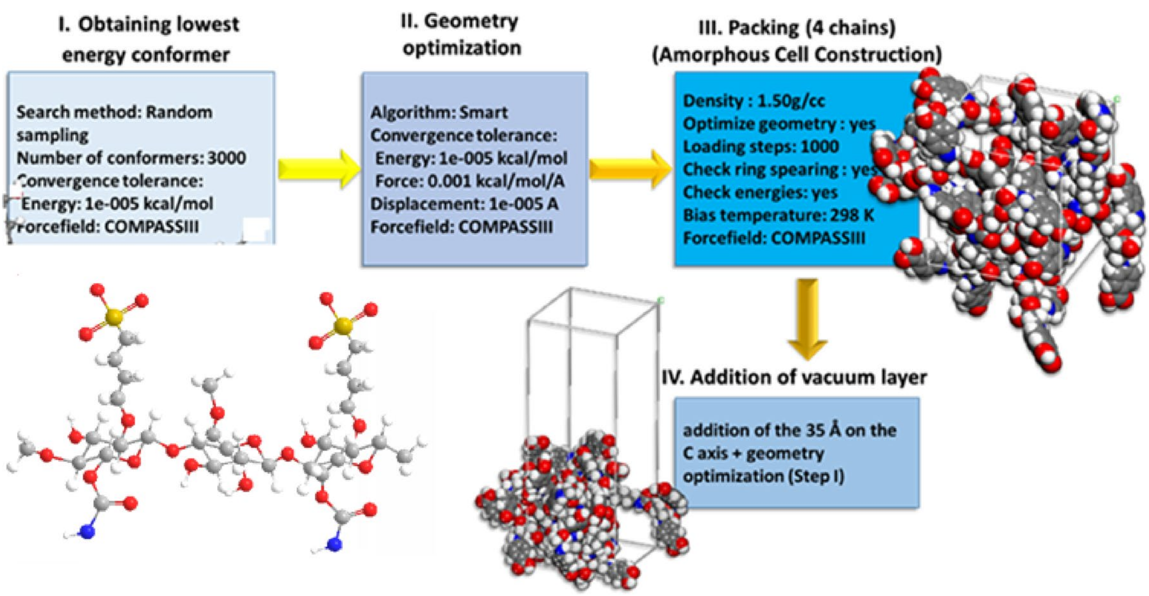

Fig. 9. The procedures and related computation information for creating the Cell-S absorbates PBC model.

ensemble with a temperature of 298.00 K utilizing Berendsen thermostat (1 fs time step with a 700 ps duration of the simulation)[65,66].

DFT
The geometries of the matching pairs of Cu(II) and adsorbent structures are depicted in Fig. 10. The interactive energy of the Cu(II) ions with both adsorbates is comparable calculated DFT. The obtained value for *Cell-BS-HDI*/Cu(II) is – 138.21 kcal/mol, while the value for and Cell-BS-PPDI /Cu(II) is – 140.72 kcal/mol.

The AIM study focused on integrating electron density over Bader atoms. Key points were identified, and local or integrated features were calculated at the bond critical points (BCPs) linking the oxygen atoms and Cu(II) cation. The results indicate that the metal–ligand Cu–O binding has a considerable amount of ionic character, which causes these ions to adsorb onto Cell-S-HMF and Cell-S-PPF adsorbents[67,68]. The presence of closed-shell interactions can be inferred from the low electron density (ρBCP approximately 0.04 a.u.) and the positive values of the Laplacian (∇2ρBCP ranging from 0.07 to 0.18 a.u.)[69].

Monte Carlo
In this study the most effective Cu(II) adsorption arrangement on the Cell-S-HMF and Cell-S-PPF surfaces must be chosen to precisely identify the various energy outputs (Fig. 10).

The computation of the adsorption energetics is made possible due to the interaction of the functional groups on the surface of polymeric chains with the Cu(II). This was computed using the formula presented in Eq. (3) (Eads) [70,71]:

$$E_{adsorption} = E_{Cell-S/\mathrm{Cu(II)}} - \left(E_{Cell-S} + E_{\mathrm{Cu(II)}}\right) \quad (3)$$

where $E_{Cell-S/\mathrm{Cu(II)}}$ is the total energy of the simulated adsorption system and $E_{Cell-S} + E_{\mathrm{Cu(II)}} is$ the total energy of the adsorbate molecules and adsorbent.

The creation of several combinations of the species (molecules, ions) used in the simulation box is the foundation of this approach to determining molecular complexity. Figure 11 shows the adsorption geometries of the most favorable or low energy adsorption sites on adsorbate surface. These binding locations were located by many Monte Carlo simulations with random parameters.

The high negative value of E_{ads} support the experimental results that indicates the high affinity of both Cell-S foams for Cu(II) ions[72–74]. The technique for determining and recording the adsorbate dynamics on the surface of the simulated material is used in MD simulations[75]. Figure 12 shows the final configuration of the adsorbate ions as they reside on the Cell-S surfaces throughout MD.

One method to guarantee that the molecules energy content is as low as is practically possible is to monitor and account for any temperature changes that occur during the MD simulation. This is one way to guarantee that

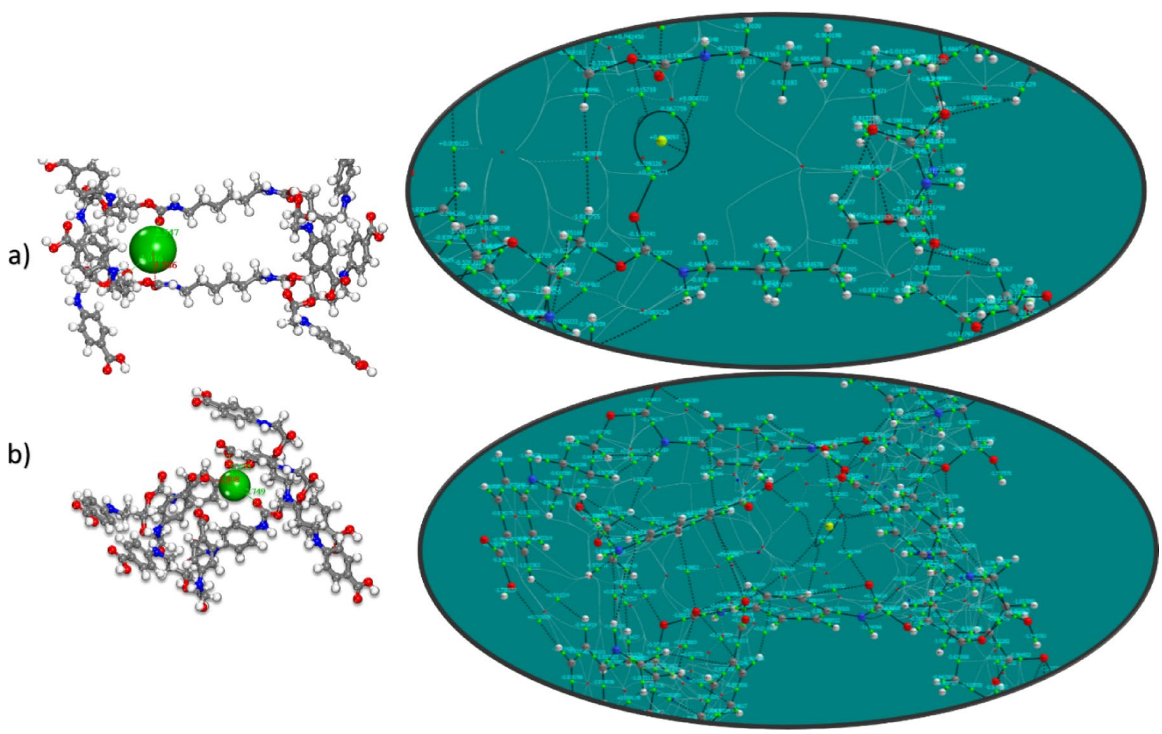

Fig. 10. Adsorbent foam/Cu(II) DFT geometries and matching molecular graphs obtained from a study using the Quantum Theory of Atoms in Molecules (QTAIM).

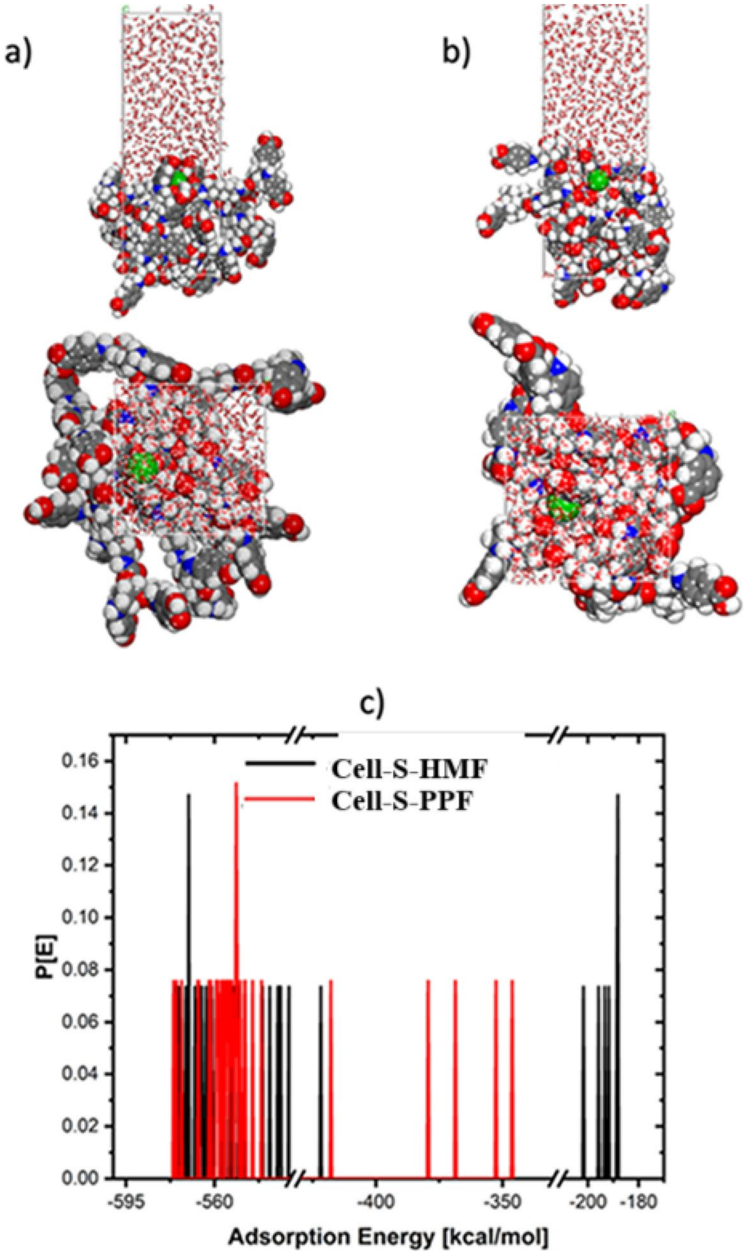

Fig. 11. (**a**) The minimal energy configuration of the simulation box derived from Monte Carlo methods and (**b**) the probability distribution of adsorption energies for Cu(II) ions on foam surfaces during Monte Carlo simulations.

the molecules energy content is as low as is practically possible[76,77]. Figure 13 shows that there is no discernible change in temperature, which is a proof that the MD used in our system was worked properly[78,79].

The strong interactions that Cu(II) ions exhibit with the adsorbate surface could be attributed to their proximity to the Cell-BS surfaces and the obtained high negative adsorption energy value[59].

Conclusion

This research successfully demonstrates the potential of cellulose-based foams as effective adsorbents for the removal of toxic metal ions from wastewater. Cellulose-based foams were efficiently prepared through the reaction of a cellulose solution in LiCl/DMAc with alkyl sulfonate, followed by crosslinking using p-phenylene diisocyanate and hexamethylene diisocyanate. The structures of the prepared foams were characterized by FT-IR and morphology was studied by SEM. Both foams showed excellent efficiency toward various metal ions present in a sample of wastewater. The optimum adsorption parameters for both foams were determined using Cu(II) as a model ion. Determined values of thermodynamic parameters indicate a spontaneous bonding of Cu(II) to the foam active sites. The obtained kinetic parameters revealed an adsorption process that obeys a pseudo second order kinetics. Theoretical computation using Molecular Dynamic (MD) and Monte Carlo

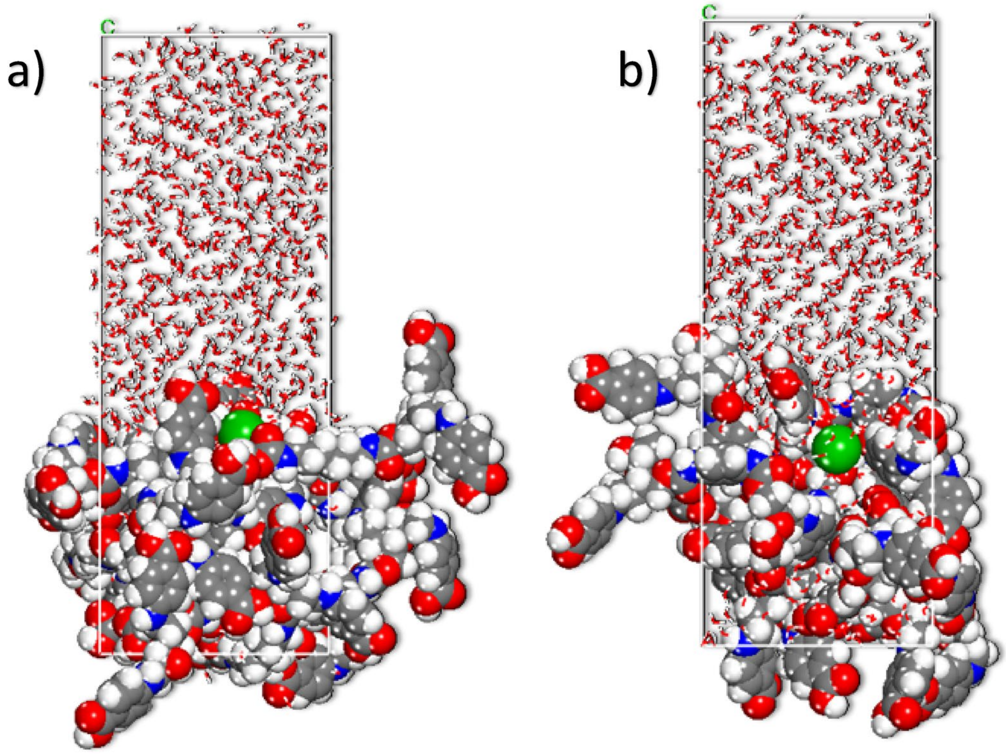

Fig. 12. The geometry of the lowest adsorption energy configurations, as obtained from molecular dynamics simulations for Cu(II) on foam surfaces, are detailed for both Cell-S-HMF and Cell-S-PPF.

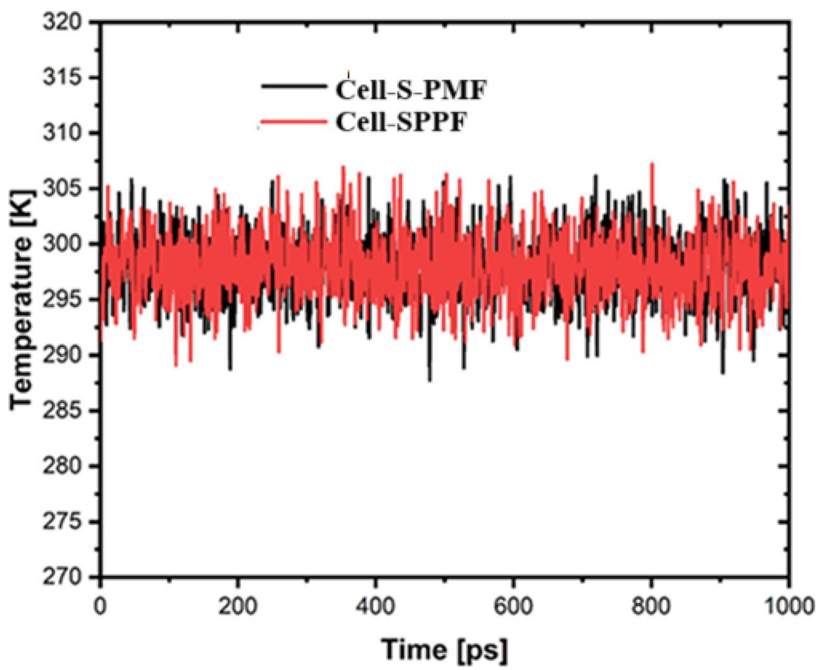

Fig. 13. Variation in temperature during the MD simulation.

(MC) simulation Models demonstrated strong affinity of generated foams for the model ion Cu(II), with highly negative adsorption energy values indicating a strong binding of Cu(II) to the foam surfaces. The findings suggest a promising avenue for the commercialization of these materials in wastewater treatment applications, leveraging their high adsorption capacity and favorable kinetics.

Data availability

The data presented in this study are available upon request from the corresponding author.

Received: 19 August 2025; Accepted: 11 November 2025
Published online: 29 December 2025

References

1. El-sharief, F. & M., Asweisi, A, A., Bader, N.,. Separation of Some Metal Ions Using β-Naphthol Modified Polyurethane Foam. *Asian J. Nanosci. Mater.* **2**, 149–158 (2019).
2. Goel. P. *Water Pollution: Causes, Effects and Control*: *New Age International* (2006).
3. Shawai, S. A. A. et al. A review on heavy metals contamination in water and soil: effects, sources and phytoremediation techniques. *Int. J. Miner. Process.* **2**, 21–27 (2017).
4. Bharathy, N. Water pollution and water quality standards for livestock. *Int. J. Sci. Environ. Technol.* **7**, 1905–1913 (2018).
5. Junior, A. C. G. et al. Adsorption of Cd (II), Pb (II) and Cr (III) on chemically modified Euterpe Oleracea biomass for the remediation of water pollution. *Acta Sci. Technol.* **43**, e50263–e50263 (2021).
6. da Paz Schiller, A. et al. Influence of hydrological flows from tropical watersheds on the dynamics of Cu and Zn in sediments. *Environ. Monit. Assess.* **191**, 1–11 (2019).
7. Masindi, V. & Muedi, K. L. Environmental contamination by heavy metals. *Heavy Met.* **10**, 115–132 (2018).
8. Sud, D., Mahajan, G. & Kaur, M. Agricultural waste material as potential adsorbent for sequestering heavy metal ions from aqueous solutions–A review. *Bioresour. Technol.* **99**, 6017–6027 (2008).
9. Abdel-Ghani, N., Hefny, M. & El-Chaghaby, G. A. Removal of lead from aqueous solution using low cost abundantly available adsorbents. *Int. J. Environ. Sci. Technol.* **4**, 67–73 (2007).
10. Alqadami, A. A., Naushad, M., AlOthman, Z. A., Alsuhybani, M. & Algamdi, M. Excellent adsorptive performance of a new nanocomposite for removal of toxic Pb (II) from aqueous environment: adsorption mechanism and modeling analysis. *J. Hazard. Mater.* **389**, 121896 (2020).
11. Sen, T. K. *Air, Gas, and Water Pollution Control Using Industrial and Agricultural Solid Wastes Adsorbents* (CRC Press, 2017).
12. Afroze, S. & Sen, T. K. A review on heavy metal ions and dye adsorption from water by agricultural solid waste adsorbents. *Water Air Soil Pollut.* **229**, 1–50 (2018).
13. Demirbas, A. Heavy metal adsorption onto agro-based waste materials: a review. *J. Hazard. Mater.* **157**, 220–229 (2008).
14. Mo, J. et al. A review on agro-industrial waste (AIW) derived adsorbents for water and wastewater treatment. *J. Environ. Manag.* **227**, 395–405 (2018).
15. Şenol, Z. M., Gül, Ü. D., Gurbanov, R. & Şimşek, S. Optimization the removal of lead ions by fungi: Explanation of the mycosorption mechanism. *J. Environ. Chem. Eng.* **9**, 104760 (2021).
16. Şenol, Z. M., Gül, Ü. D. & Şimşek, S. Assessment of Pb^{2+} removal capacity of lichen (*Evernia prunastri*): Application of adsorption kinetic, isotherm models, and thermodynamics. *Environ. Sci. Pollut. Res.* **26**, 27002–27013 (2019).
17. Jodeh, S. et al. Magnetic nanocellulose from olive industry solid waste for the effective removal of methylene blue from wastewater. *Environ. Sci. Pollut. Res.* **25**, 22060–22074 (2018).
18. Kumari, B. et al. A two-in-one thiosemicarbazide and whole pine needle-based adsorbent for rapid and efficient adsorption of methylene blue dye and mercuric ions. *Environ. Sci. Pollut. Res.* **31**, 21591–21609. https://doi.org/10.1007/s11356-024-32446-3 (2024).
19. Akkermans, R. L. C., Spenley, N. A. & Robertson, S. H. COMPASS III: Automated fitting workflows and extension to ionic liquids. *Mol. Simul.* **47**(7), 540–551 (2021).
20. Chauhan, S. et al. Tailoring of spherical nanocellulose via esterification with methionine followed by protonation to generate two different adsorbents for mercuric ions and Congo red. *Int. J. Biol. Macromol.* **279**(20), 135313. https://doi.org/10.1016/j.ijbiomac.2024.135313 (2024).
21. Chauhan, S. et al. Tailoring of spherical nanocellulose via esterification with methionine followed by protonation to generate two different adsorbents for mercuric ions and Congo red. *Int. J. Biol. Macromol.* **279**, 135313. https://doi.org/10.1016/j.ijbiomac.2024.135313 (2024).
22. Berisha, A. Unraveling the electronic influence and nature of covalent bonding of aryl and alkyl radicals on the B12N12 nanocage cluster. *Sci. Rep.* **13**(1), 1–11. https://doi.org/10.1038/s41598-023-28055-8 (2023).
23. Ben Hadj Ayed, M. et al. Structures and relative stabilities of Na+Ne n (n = 1–16) clusters via pairwise and DFT calculations. *Theor. Chem. Acc.* https://doi.org/10.1007/s00214-019-2476-4 (2019).
24. Chakraborty, R., Asthana, A., Singh, A. K., Jain, B. & Susan, A. B. H. Adsorption of heavy metal ions by various low-cost adsorbents: A review. *Int. J. Environ. Anal. Chem.* **102**, 342–379 (2022).
25. Karnitz, O. Jr. et al. Adsorption of heavy metal ion from aqueous single metal solution by chemically modified sugarcane bagasse. *Bioresour. Technol.* **98**, 1291–1297 (2007).
26. Doan, H., Lohi, A., Dang, A. & Dang-Vu, T. Removal of Zn^{+2} and Ni^{+2} by adsorption in a fixed bed of wheat straw. *Process Saf. Environ. Prot.* **86**, 259–267 (2008).
27. Acar, F. & N., Eren, Z.,. Removal of Cu (II) ions by activated poplar sawdust (Samsun Clone) from aqueous solutions. *J. Hazard. Mater.* **137**, 909–914 (2006).
28. Vieira, M., de Almeida Neto, A., Da Silva, M., Carneiro, C. & Melo Filho, M. Adsorption of lead and copper ions from aqueous effluents on rice husk ash in a dynamic system. *Braz. J. Chem. Eng.* **31**, 519–529 (2014).
29. Hamed, O. A., Foad, Y., Hamed, E. M. & Al-Hajj, N. Cellulose powder from olive industry solid waste. *BioResources* **7**, 4190–4201 (2012).
30. Hamed, O. A. et al. Cellulose acetate from biomass waste of olive industry. *J. Wood Sci.* **61**, 45–52 (2015).
31. Chauhan, K. et al. Dibutyltin dilaurate catalyzed guar gum and toluene diisocyanate polyurethane foam for the removal of malachite green from wastewater. *Polym. Int.* **74**(4), 307–323. https://doi.org/10.1002/pi.6722 (2025).
32. Hong, H.-J. et al. Carboxymethlyated cellulose nanofibrils (CMCNFs) embedded in polyurethane foam as a modular adsorbent of heavy metal ions. *Carbohydr. Polym.* **195**, 136–142 (2018).
33. Lemos, V. et al. Application of polyurethane foam as a sorbent for trace metal pre-concentration—a review. *Spectrochim Acta Part B* **62**, 4–12 (2007).
34. Anthemidis, A., Zachariadis, G. A. & Stratis, J. A. On-line preconcentration and determination of copper, lead and chromium (VI) using unloaded polyurethane foam packed column by flame atomic absorption spectrometry in natural waters and biological samples. *Talanta* **58**, 831–840 (2002).
35. Azeem, S. A., Attaf, S. M. & El-Shahat, M. Acetylacetone phenylhydrazone functionalized polyurethane foam: Determination of copper, zinc and manganese in environmental samples and pharmaceutics using flame atomic absorption spectrometry. *React. Funct. Polym.* **73**, 182–191 (2013).
36. Jamwal, P., Chauhan, S., Kumar, K. & Chauhan, G. S. Fabricating pine needles derived spherical nanocellulose with polyaniline and montmorillonite clay for simultaneous removal of cationic and anionic dyes from binary mixtures. *Int. J. Biol. Macromol.* **301**, 140340. https://doi.org/10.1016/j.ijbiomac.2025.140340 (2025).

37. Chauhan, S. et al. A highly efficient and green adsorbent for anionic dyes synthesized from whole pine needles modified with glycidyltrimethylammonium chloride: Synthesis, kinetic, and thermodynamic investigation. *Biomass Conv. Bioref.* **14**, 31413–31429. https://doi.org/10.1007/s13399-023-04776-8 (2024).
38. Salam, S. Chemically modified polyurethane foam for pre-concentration and separation of inorganic and organic species. *Citeseer* (2008).
39. Dacewicz, E. & Grzybowska-Pietras, J. Polyurethane foams for domestic sewage treatment. *Materials* **14**, 933 (2021).
40. Kumari, S., Chauhan, G. S. & Ahn, J. H. Novel cellulose nanowhiskers-based polyurethane foam for rapid and persistent removal of methylene blue from its aqueous solutions. *J. Chem. Eng.* **304**, 728–736 (2016).
41. Ngah, W. W., Teong, L. & Hanafiah, M. M. Adsorption of dyes and heavy metal ions by chitosan composites: A review. *Carbohyd. Polym.* **83**(4), 1446–1456. https://doi.org/10.1016/j.carbpol.2010.11.004 (2011).
42. Crini, G., Peindy, H. N., Gimbert, F. & Robert, C. Removal of C.I. Basic Green 4 (Malachite Green) from aqueous solutions by adsorption using cyclodextrin-based adsorbent: Kinetic and equilibrium studies. *Sep. Purif. Technol.* **53**(1), 97–110. https://doi.org/10.1016/j.seppur.2006.06.018 (2007).
43. Tiwari, A., Tapadia, K., Thakur, C. & Sharma, A. A sustainable approach to Gilloy-shoot extract-mediated synthesis of magnetite nanoparticles: isotherm and kinetic study of U(VI) removal. *J. Radioanal. Nucl. Chem* https://doi.org/10.1007/s10967-022-08441-8 (2022).
44. Kannan, N. & Meenakshisundaram, M. adsorption of congo red on various activated carbons a comparative study. *Water Air Soil Pollut.* **138**(1–4), 289–305 (2002).
45. Klamt, A. *COSMO-RS: From Quantum Chemistry To Fluid Phase Thermodynamics and Drug Design* (Elsevier, 2005).
46. Klamt, A. The COSMO and COSMO-RS solvation models. *Rev. Comput. Mol. Sci.* **8**, e1338 (2018).
47. Berisha, A. Interactions between the aryldiazonium cations and graphene oxide: a DFT study. *J. Chem.* **2019**, 5126071 (2019).
48. Jessima, S. H. M. et al. Corrosion mitigation performance of disodium EDTA functionalized chitosan biomacromolecule-Experimental and theoretical approach. *Int. J. Biol. Macromol.* **178**, 477–491 (2021).
49. Rbaa, M. et al. New Epoxy sugar based glucose derivatives as eco friendly corrosion inhibitors for the carbon steel in 1.0 M HCl: Experimental and theoretical investigations. *J. Alloys Compd.* **833**, 154949 (2020).
50. Hsissou, R. et al. Novel derivative epoxy resin TGETET as a corrosion inhibition of E24 carbon steel in 1.0 M HCl solution. Experimental and computational (DFT and MD simulations) methods. *J. Mol. Liq.* **284**, 182–192 (2019).
51. Berisha, A. Experimental, Monte Carlo and molecular dynamic study on corrosion inhibition of mild steel by pyridine derivatives in aqueous perchloric acid. *Electrochem.* **1**, 188–199 (2020).
52. Amrhar, O., Berisha, A., El Gana, L., Nassali, H., Elyoubi, M. S. Removal of methylene blue dye by adsorption onto Natural Muscovite Clay: experimental, theoretical and computational investigation. *Int. J. Environ. Anal. Chem.* 1–26 (2021).
53. Hamed, O. A. et al. Cellulose powder functionalized with phenyl biguanide: Synthesis, cross-linking, metal adsorption, and molecular docking. *BioResources* **16**, 7263–7282 (2021).
54. Khalaf, B. et al. Cellulose-based hectocycle nanopolymers: Synthesis, molecular docking and adsorption of difenoconazole from aqueous medium. *Int. J. Mol. Sci.* **22**, 6090 (2021).
55. Babas, H. et al. Sofosbuvir adsorption onto activated carbon derived from argan shell residue: Optimization, kinetic, thermodynamic and theoretical approaches. *J. Mol. Liq.* **356**, 119019 (2022).
56. Hasani, N. et al. Theoretical, equilibrium, kinetics and thermodynamic investigations of methylene blue adsorption onto lignite coal. *Molecules* **2022**, 27 (1856).
57. Hamed, O. et al. Synthesis of a cross-linked cellulose-based amine polymer and its application in wastewater purification. *Environ. Sci. Pollut. Res.* **26**, 28080–28091 (2019).
58. LazaroMartinez, J. M., Romasanta, P. N., Chattah, A. K. & Buldain, G. Y. NMR characterization of hydrate and aldehyde forms of imidazole-2-carboxaldehyde and derivatives. *JOC* **75**, 3208–3213 (2010).
59. Iqhrammullah, M. et al. Characterization and performance evaluation of cellulose acetate–polyurethane film for lead II ion removal. *Polymers* **12**, 1317 (2020).
60. Kim, U.-J. et al. Protein adsorption of dialdehyde cellulose-crosslinked chitosan with high amino group contents. *Carbohydr. Polym.* **163**, 34–42 (2017).
61. Pino-Rios, R., Chigo-Anota, E., Shakerzadeh, E. & Cárdenas-Jirón, G. B12N12 cluster as a collector of noble gases: A quantum chemical study. *Phys. E Low-Dimens. Syst. Nanostructures* **115**, 113697 (2020).
62. Anirudhan, T. & Sreekumari, S. Adsorptive removal of heavy metal ions from industrial effluents using activated carbon derived from waste coconut buttons. *J. Environ. Sci.* **23**, 1989–1998 (2011).
63. Gül, Ü. D., Şenol, Z. M., Gürsoy, N. & Şimşek, S. Effective UO_2^{2+} removal from aqueous solutions using lichen biomass as a natural and low-cost biosorbent. *J. Environ. Radioact.* **205**, 93–100 (2019).
64. Uddin, M. K. A review on the adsorption of heavy metals by clay minerals, with special focus on the past decade. *J. Chem. Eng.* **308**, 438–462 (2017).
65. Adeyemo, A., Adeoye, I. O. & Bello, O. S. Adsorption of dyes using different types of clay: A review. *Appl. Water Sci.* **7**, 543–568 (2017).
66. Bo, S. et al. Flexible and porous cellulose aerogels/zeolitic imidazolate framework (ZIF-8) hybrids for adsorption removal of Cr (IV) from water. *J. Solid State Chem.* **262**, 135–141 (2018).
67. Chwastowski, J., Staroń, P., Kołoczek, H. & Banach, M. Adsorption of hexavalent chromium from aqueous solutions using Canadian peat and coconut fiber. *J. Mol. Liq.* **248**, 981–989 (2017).
68. Lin, J. et al. Durably antibacterial and bacterially antiadhesive cotton fabrics coated by cationic fluorinated polymers. *ACS Appl. Mater. Interfaces.* **10**, 6124–6136 (2018).
69. Lin, J., Zhan, S., Fang, M., Qian, X. & Yang, H. Adsorption of basic dye from aqueous solution onto fly ash. *J. Environ. Manag.* **87**, 193–200 (2008).
70. Gupta, S. & Babu, B. Utilization of waste product (tamarind seeds) for the removal of Cr (VI) from aqueous solutions: equilibrium, kinetics, and regeneration studies. *J. Environ. Manag.* **90**, 3013–3022 (2009).
71. Mahmoudi, G. et al. Tetrel bonding and other non-covalent interactions assisted supramolecular aggregation in a new Pb (II) complex of an isonicotinohydrazide. *Molecules* **25**, 4056 (2020).
72. Kowalik, M., Masternak, J., Brzeski, J., Daszkiewicz, M. & Barszcz, B. Effect of a lone electron pair and tetrel interactions on the structure of Pb (II) CPs constructed from pyrimidine carboxylates and auxiliary inorganic ions. *Polyhedron* **219**, 115818 (2022).
73. Moncomble, A., Cornard, J.-P. & Meyer, M. A quantum chemistry evaluation of the stereochemical activity of the lone pair in PbII complexes with sequestering ligands. *J. Mol. Model.* **23**, 1–13 (2017).
74. Guo, L., Zhang, S., Li, W., Hu, G. & Li, X. Experimental and computational studies of two antibacterial drugs as corrosion inhibitors for mild steel in acid media. *Mater. Corros.* **65**, 935–942 (2014).
75. Hsissou, R. et al. Anticorrosive property of hexafunctional epoxy polymer HGTMDAE for E24 carbon steel corrosion in 1.0 M HCl: Gravimetric, electrochemical, surface morphology and molecular dynamic simulations. *Polym. Bull.* **77**, 3577–3601 (2020).
76. Dagdag, O. et al. et Polymeric-based epoxy cured with a polyaminoamide as an anticorrosive coating for aluminum 2024–T3 surface: Experimental studies supported by computational modeling. *J. Bio- Tribo-Corros.* **5**, 1–13 (2019).
77. Abbout, S. et al. Galactomannan as a new bio-sourced corrosion inhibitor for iron in acidic media. *Heliyon* **6**, e03574 (2020).
78. Dagdag, O. et al. Fabrication of polymer based epoxy resin as effective anti-corrosive coating for steel: Computational modeling reinforced experimental studies. *Surf. Interfaces* **18**, 100454 (2020).

79. Nairat, N. et al. Cellulose polymers with β-amino ester pendant group: design, synthesis, molecular docking and application in adsorption of toxic metals from wastewater. *BMC Chem.* **16**, 1–21 (2022).

Acknowledgements
This study was supported by The Scientific and Technological Research Council of Turkey (TUBITAK) and The Higher Council for Innovation and Excellence of Palestine (HCIE), 2521 International Bilateral Research Project (Grant Number: 120N633), and the authors gratefully acknowledge TUBITAK and HCIE. The authors gratefully acknowledging the support from the Ministry of Education, Science and Technology of Kosovo (Nr.2-5069) for providing computing resources.

Author contributions
Data curation, A.B.; O. N., Investigation, O.H, BA, D.S.; Methodology, O.H., A.D.; Software, A.B..; writing—original draft preparation, O.H., B.A. Writing—review and editing, W.M. A.B., O.D.; S. J., editing and submitting. All authors have read and agreed to the published version of the manuscript.

Funding
This study was supported by The Scientific and Technological Research Council of Turkey (TUBITAK) and the Higher Council for Innovation and Excellence of Palestine (HCIE), 2521 International Bilateral Research Project (Grant Number: 120N633), and the authors gratefully acknowledge TUBITAK and HCIE. This support was for purchasing chemicals and do analysis.

Declarations

Competing interests
The authors declare no competing interests.

Informed consent
The data presented in this study are available on request from the corresponding author.

Additional information
Supplementary Information The online version contains supplementary material available at https://doi.org/10.1038/s41598-025-28450-3.

Correspondence and requests for materials should be addressed to O.H., W.M. or S.J.